Impaired hemoglobin clearance by sinusoidal endothelium promotes vaso-occlusion and liver injury in sickle cell disease

Tomasz W. Kaminski,[1*°] Omika Katoch,[1*°] Ziming Li,[1] Corrine B. Hanway,[1] Rikesh K. Dubey,[1°] Adekunle Alagbe,[1] Tomasz Brzoska,[1] Hong Zhang,[2] Prithu Sundd,[1,3,4°] Gregory J. Kato,[5] Enrico M. Novelli[1,6] and Tirthadipa Pradhan-Sundd[1,6°]

[1]Pittsburgh Heart, Lung and Blood Vascular Medicine Institute, University of Pittsburgh School of Medicine, Pittsburgh, PA; [2]BioMagis Inc., San Diego, CA; [3]Department of Bioengineering, University of Pittsburgh, Pittsburgh, PA; [4]Division of Pulmonary Allergy and Critical Care Medicine, Department of Medicine, University of Pittsburgh School of Medicine, Pittsburgh, PA and [5]CSL Behring, King of Prussia, PA and [6]Division of Hematology/Oncology, Department of Medicine, University of Pittsburgh School of Medicine, Pittsburgh, PA, USA

**TWK and OK contributed equally as first authors.*
°Current address: Versiti Blood Research Institute and Medical College of Wisconsin, Milwaukee, WI, USA

Correspondence: Tirthadipa Pradhan-Sundd
tip9@pitt.edu
tpradhan@versiti.org

Received: June 21, 2023.
Accepted: November 2, 2023.
Early view: November 9, 2023.

https://doi.org/10.3324/haematol.2023.283792

Supplemental Material For

Title: Impaired hemoglobin clearance by sinusoidal endothelium promotes vaso-occlusion and liver injury in sickle cell disease

Authors:

Authors: Tomasz W Kaminski[1#], Omika Katoch[1#], Ziming Li[1], Corrine B Hanway[1], Rikesh K Dubey[1], Adekunle Alagbe[1,] Tomasz Brzoska[1,] , Hong Zhang[3], Prithu Sundd[1, 4,5], Gregory J Kato[6], Enrico M Novelli[1, 7], Tirthadipa Pradhan-Sundd[1, 7, *].

1. Pittsburgh Heart, Lung and Blood Vascular Medicine Institute, University of Pittsburgh School of Medicine, Pittsburgh, PA, USA.
2. Biomagis. Inc, USA.
3. Department of Bioengineering, University of Pittsburgh, Pittsburgh, PA, USA.
4. Division of Pulmonary Allergy and Critical Care Medicine, Department of Medicine, University of Pittsburgh School of Medicine, Pittsburgh, PA, USA.
5. CSH, Behring, USA
6. Division of Hematology/Oncology, Department of Medicine, University of Pittsburgh School of Medicine, Pittsburgh, PA, USA.

# these authors have contributed equally.

*To whom correspondence should be addressed:

Tirthadipa Pradhan-Sundd, PhD

Vascular Medicine Institute

Department of Medicine

Division of Hematology-Oncology

University of Pittsburgh School of Medicine

200 Lothrop Street, Pittsburgh, PA, 15261

Email: tip9@pitt.edu

Content:

Supplemental Methods

Histology, immunohistochemistry (IHC) and immunofluorescence (IF): Tissue sections (4-6μm) were stained with hematoxylin and eosin (H&E), Sirius red and Prussian blue. IHC on paraffin-embedded sections was performed on livers as described elsewhere[1]. For IF, frozen liver sections were used. Primary and secondary antibodies used are mentioned in table S1. Nikon A1 Spectral Confocal microscopes were used to capture images. Nikon NIS software was used to analyze the data.

Scanning electron microscopy (SEM): Whole liver was collected from control (AS), SCD, SCD;Selp-/-, SCD+clodronate mice for SEM imaging. Slices of whole liver were fixed in 2.5% glutaraldehyde in PBS (pH 7.4) for 10 min. Tissue samples were washed thoroughly in PBS for 15 min. Tissues were then fixed in 1% Osmium tetraoxide (OsO4) in PBS for 60 min. Samples were dehydrated with different concentration of ethanol (30%, 50%, 70%, 90%) for 15 min and then samples were critical point dried. Samples were visualized using Field Emission Scanning Electron Microscope (JEOL JSM6335F) at the magnification of 10,000X to 30,000X.

Western Blotting: Immunoblotting was performed as described elsewhere[2]. The % gels were 4% to 12%. Gels were purchased from ThermoFisher Scientific(Bolt™ 4 to 12%, Bis-Tris, 1.0 mm; catalog number: NW04122BOX). The membranes used were from ThermoFisher Scientific (Nitrocellulose/Filter Paper Sandwich, 0.2 μm, 8.3 x 7.3 cm; catalog number: LC2000). In some cases, proteins were reprobed after stripping on the same membrane with a different antibody to detect another protein of interest of different size. The following primary antibodies used are mentioned in table S2. Membranes were 4 washed five times for 5m each in TBST before being probed with HRP–conjugated secondary antibodies (1:5000 diluted in TBST; Santa Cruz

Biotechnology) for 1.5h at room temperature. Membranes were washed three times for 10m each in TBST and visualized using the Enhanced Chemiluminescence System (GE Healthcare). AF647 tagged Hb and FITC and AF647 tagged HbS was purchased from BioImagis, USA.

Serum biochemistry: Total bilirubin, direct bilirubin, aspartate aminotransferase (AST), and alanine aminotransferase (ALT) were measured in serum samples taken before sacrifice. Serum biochemistry was measured by automated testing in the Clinical Chemistry Division, University of Pittsburgh school of medicine.

mRNA isolation and real time polymerase chain reaction: mRNA was isolated and purified from livers of AS and SCD mice (n=3/group). mRNA was isolated using Trizol (Invitrogen). RT-PCR was performed as described elsewhere[3]. The method for calculating the transcripts was delta-delta Ct method (2^–ΔΔCt). Changes in target mRNA were normalized to GAPDH mRNA for each sample and presented as fold-change over the average the respective control group. Each sample was run in triplicate. Sequences of primers used in this study are available on table S3.

Liver perfusion: For liver perfusion we followed the protocol described here[4]. Briefly, mice were anesthetized by intraperitoneal injection of anesthesia cocktail (100 mg/kg ketamine HCl and 20 mg/kg xylazine). Following anesthesia, the inferior vena cava is cannulated with the needle connected with tubing filled with perfusion buffer (HBSS no Ca2+ no Mg2+ no phenol red, 0.5mM EDTA and 25mM HEPES). After cannulation, cut the portal vein once appearance of portal vein swelling. Liver was perfused with the perfusion buffer to chelate calcium and wash out blood and other circulating cells. Then the 2.0 % PFA was used until the liver appears beige and then liver slices placed in 2.5% glutaraldehyde (for TEM and SEM analysis). For cell separation, liver was perfused in collagenase instead of PFA.

Hepatocyte -non-hepatocyte isolation: The livers were perfused as mentioned above using peristaltic pump. Excised liver was minced, filtered through 70 uM filter and centrifuged at 50 g for 2 min for hepatocytes fraction. Supernatant containing non-hepatocytes were separated by centrifuging at 500 g for 5 min. Live cells from both the fractions were collected after centrifugation at 100 g for 10 min in 36% percoll solution (Sigma-Aldrich).

Clodronate-Liposome treatment: A low dose of clodronate liposome (50-100 ul/ mouse; approx. body weight 25 gms) was used to deplete monocytes. A high dose (100-200ul/mouse) was used to deplete hepatic Kupffer cells. Mice were sacrificed 24-72 hrs. post injection.

Drug treatments: For iron dextran treatment, control (AS) and SCD mice were administered intra-peritoneally with ten doses (one dose every second day) of 100mg/kg b.w. of Iron dextran (Sigma D8517-25ML). Mice were sacrificed after 3 weeks and liver and blood samples were collected for further analysis.

Image Analysis: Movies were processed using Nikon's NIS Elements (Nikon Elements 3.10). A median filter with a kernel size of 3 was applied over each video frame to improve signal-to-noise ratio. Signal contrast in each channel of a multicolor image was further enhanced by adjusting the maxima and minima of the intensity histogram of that channel. For measurements of colocalization between two proteins, images were analyzed with NLS software (Nikon Elements 3.10). Colocalization was measured by finding the Pearson coefficient of six different images (N=3). Pearson's coefficient represents the intensity correlation of all nonzero pixels that overlay in images of two channels.

Method References:

1. Vats R, Li Z, Ju EM, et al. Intravital imaging reveals inflammation as a dominant pathophysiology of agerelated hepatovascular changes. *Am J Physiol - Cell Physiol*. Published online 2022. doi:10.1152/ajpcell.00408.2021

2. Pradhan-Sundd T, Vats R, Russell JO, et al. Dysregulated Bile Transporters and Impaired Tight Junctions During Chronic Liver Injury in Mice. *Gastroenterology*. Published online 2018. doi:10.1053/j.gastro.2018.06.048

3. Pradhan-Sundd T, Zhou L, Vats R, et al. Dual catenin loss in murine liver causes tight junctional deregulation and progressive intrahepatic cholestasis. *Hepatology*. Published online October 10, 2017. doi:10.1002/hep.29585

4. Jung Y, Zhao M, Svensson KJ. Isolation, culture, and functional analysis of hepatocytes from mice with fatty liver disease. *STAR Protoc*. Published online 2020. doi:10.1016/j.xpro.2020.100222

5. Jimenez MA, Tutuncuoglu E, Barge S, Novelli EM, Sundd P. Quantitative microfluidic fluorescence microscopy to study vaso-occlusion in sickle cell disease. *Haematologica*. Published online 2015. doi:10.3324/haematol.2015.126631

SUPPLEMENTAL TABLES WITH LEGENDS

Table S1: List of antibodies used for immunohistochemical assays.

Primary Antibody for IHC/IF				
Name	Concentration	Company		Orig concentration
CD31	1:100 dilution	Dianova	DIA-310	0,2 mg/mL
P21 (new)	1:100 dilution	Proteintech	28248-1-AP	500 µg/mL
P53	1:100 dilution	Cell Signaling Technology	2524T	
lyve1	1:100 dilution	ReliaTech GmbH	103-PA50	1.0 mg/mL.
Hb-AF647	1:100 dilution	Biomagnis	lot# C101006	0.85 mg/mL
MFG8	1:100 dilution	Invitrogen	PA5-109955	1.65 mg/mL
CLEF4C	1:100 dilution	R&D Systems	AF2784	0.2 mg/mL
CD11b	1:100 dilution	Novus Biologicals	NB110-89474SS	1 mg/mL

Table S2: List of antibodies used for Western blot.

Western Blot	Concentration used			Orig concentration
Hb-A2	1.203 µg/mL	anclonal	A8427	1.203 mg/mL
GAPDH	0.042 µg/mL	Cell Signaling Technology, Inc.	2118L	42 µg/mL
p53	0.313 µg/mL	Cell Signaling Technology, Inc.	2524S	313 µg/mL
p21	0.5 mg/mL	Protein tech	28248-1-AP	500 mg/mL
p16	0.2 µg/mL	Santa Cruz Biotechnology	sc-81157	200 µg/mL
clef4c	0.1 µg/mL	R&D Systems	AF2784	
ferritin	0.07 µg/ml	abcam	ab75973	
F4/80 (D2S9R) XP Rabbit mAb	0.435 µg/ml	Cell Signaling Technology, Inc.	70076S	
CD11b	1µg/mL	NOVUS biotechne	NB110-89474SS	

Table S3: List of antibodies used for Intravital imaging.

Name	**Company**	**cat #**	**Concentration**
CD31	Biolegend	102414	5ug/mouse
p21	Abcam	ab237264	5ug/mouse

Table S4: List of primer sequences used in the RT-PCR assays.

Primer Sequences		
Name	Forward Sequence	Reverse Sequence
P53	AGAGTCTATAGGCCCACCCC	GCTCGACGCTAGGATCTGAC
P21	TTGCACTCTGGTGTCTGAGC	TCTGCGCTTGGAGTGATAGA
P16	GCTCAACTACGGTGCAGATTC	GCACGATGTCTTGATGTCCC
ϒH2AX	CGGTGGGCTTGAAGGTTAGT	ACTGGTATGAGGCCAGCAAC
VCAM1	CCGGCATATACGAGTGTGAAT	ATGGCAGGTATTACCAAGGAAGAT
ICAM1	GTTTAAAAACCAGACCCTCCAACT	CGTCTGCAGGTCATCTTAGGAG
INOS	CTATCAGGAAGAAATGCAGGAGAT	GAGCACGCTGAGTACCTCATT
CD31	GTGCTCTATGCAAGCCTCCA	TTCGAGGTGGTGC TGATGTC
SRA1	ATGAACAAGAGGATGCTGAC	CAAACACAAGGAGGTAGAGAG
stabilin 1	CCACTCCAAATGAAGACTTG	CTACTCATGTGGTTACGATTC
stabilin 2	GCTGCAAGTCCTCATGTCCT	TTCTGTGGCACAAACAGGGT
CR3	ATGGACGCTGATGGCAATACC	TCCCCATTCACGTCTCCCA
FCGR1	AGGTTCCTCAATGCCAAGTGA	GCGACCTCCGAATCTGAAGA
MR	CTCTGTTCAGCTATTGGACGC	CGGAATTTCTGGGATTCAGCTTC
Clec	GGAAAGTCATTCCAGACCCA	AAGACGCCATTTAACCCACA
Macro	TTAGCAGCTATGGAGGTGGC	GACACACTGATGACCTCTCGG
Siglec1	GTCTCCAGGAAGGTGGTCAG	CAGGGCTGATACTGGCTTCT
SCRAB1	TCTGGCGCTTTTTCTATCGT	ACGGCCCATACCTCTAGCTT
CD36	GATGACGTGGCAAAGAACAG	TCCTCGGGGTCCTGAGTTAT
LOX1	GAGCTGCAAACTTTTCAGG	GTCTTTCATGCAGCAACAG
18S	CGGCTACCACATCCAAGGAA	GCTGGAATTACCGCGGCT
GAPDH	GACAGTCAGCCGCATCTTCT	TTAAAAGCAGCCCTGGTGAC

Table S5: List of reagents used in *in vitro* assays.

Antibodies	Clone	company	
Alexa 488 anti-mouse CD31 antibody	MEC13.3	BioLegend	Cat#: 102513
Brilliant VioleBrilliant Violet 421™ anti-mouse CD31 Antibody	390	BioLegend	Cat#: 102423
Anti-HBA2 Rabbit pAb antibody	N/A	Abclonal	A8427
Calcium free apoptotic-dead cell tag 488	N/A	BioMagis	Cat#: 302104
Calcium free apoptotic-dead cell tag Atto 647	N/A	BioMagis	Cat#: 302111
Nystatin	N/A	Sigma	Cat#: N9150
Latrunculin-A	N/A	Thermo fisher	Cat#L12370
TNFa	N/A		
HBB rabit polyclonal A	N/A	Proteintech	16216-1-AP
Anti-Hemoglobin S (HbS)	57-8	DiaPharm	IQP-574F
HbS protein tagged with AF567 or FITC	NA	Biolegend	NA
HB protein tagged with FITC or AF647	NA	Biolegend	NA
Cells:			
C57BL/6 Mouse Liver Sinusoidal Endothelial C		Accegen	AGK4398
Human Hepatic Sinusoidal Endothelial Cells (HHSEC, Adult)		iXcells Biotechnologies	10HU-021
Endothelial cell growth medium		iXcells Biotechnologies	MD-0010
Human Lung Microvascular Endothelial Cells		Lonza	CC-2527 ?
Endothelial cell growth medium		Lonza	CC-3162
Proteins			
Normal Hemoglobin		Sigma	9008-02-0
Sickle Hemoglobin		Sigma	9035-22-7

SUPPLEMENTAL FIGURES WITH LEGENDS

Figure S1

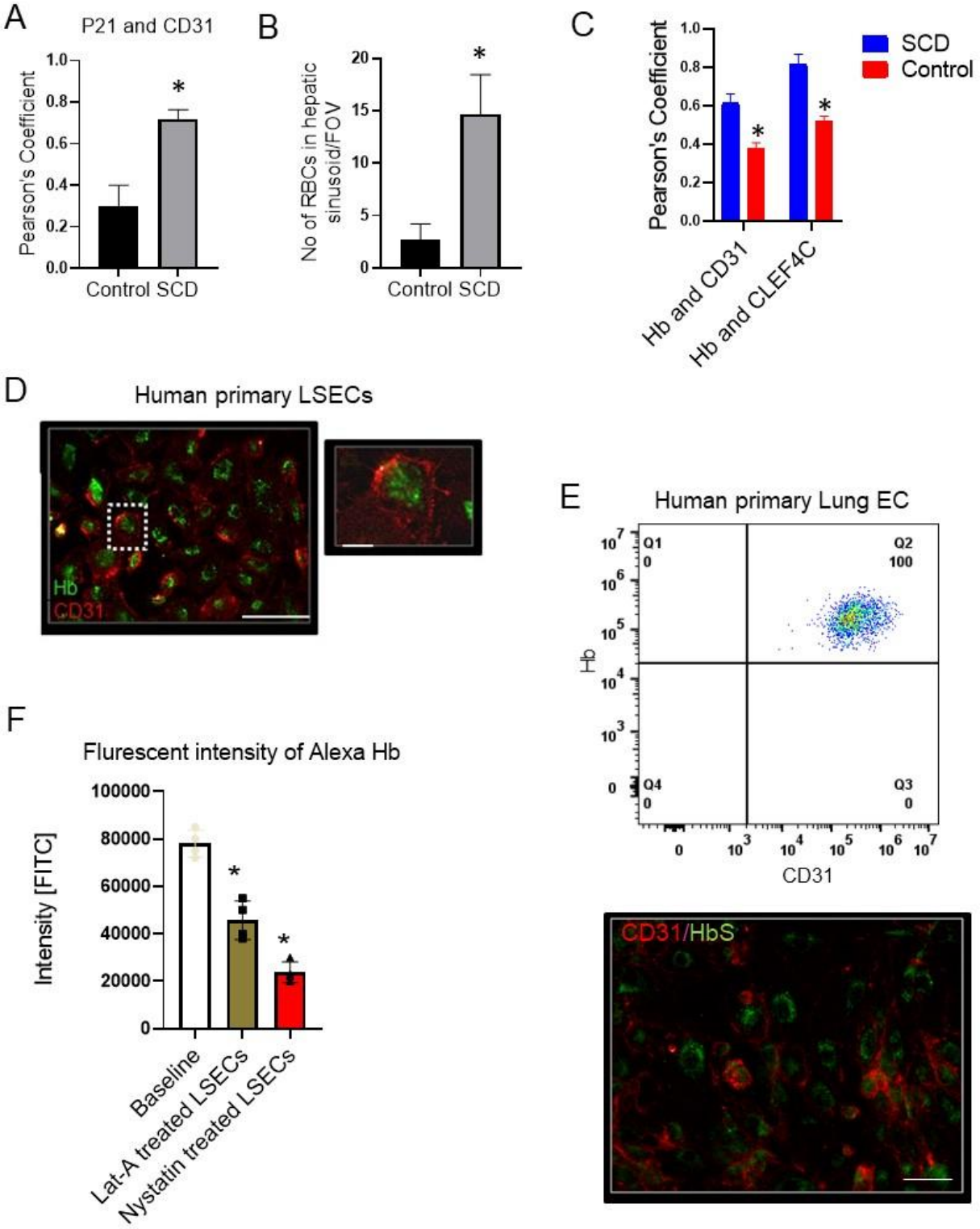
A
P21 and CD31
Pearson's Coefficient
1.0
0.8
0.6
0.4
0.2
0.0
*
Control SCD
B
No of RBCs in hepatic sinusoid/FOV
20
15
10
5
0
*
Control SCD
C
Pearson's Coefficient
1.0
0.8
0.6
0.4
0.2
0.0
SCD
Control
*
*
Hb and CD31
Hb and CLEF4C
D
Human primary LSECs
Hb
CD31
E
Human primary Lung EC
Q1
0
Q2
100
Q4
0
Q3
0
Hb
CD31
CD31/HbS
F
Flurescent intensity of Alexa Hb
Intensity [FITC]
100000
80000
60000
40000
20000
0
*
*
Baseline
Lat-A treated LSECs
Nystatin treated LSECs

Figure S1:Primary endothelial cells are capable of internalizing hemoglobin in vitro. **(A)** Quantification of colocalization (by measuring Pearson's coefficient) observed in control and SCD mouse liver tissue. Bar graph shows the increased colocalization of senescence marker P21 with liver sinusoidal endothelial cell marker CD31 in SCD mouse liver as compared to control mouse liver. **(B)** Quantification of number of RBCs found in the hepatic sinusoids of SCD and control liver tissue /FOV. FOV size ~ μm^2. **(C)** Quantification of colocalization (by measuring Pearson's coefficient) observed in control and SCD mouse liver tissue. Bar graph shows the increased colocalization of hemoglobin with liver sinusoidal endothelial cell marker CD31 and macrophage marker CLEC4F in SCD mouse liver as compared to control mouse liver. **(D)** Representative IF images showing Hb and CD31 localization in human primary LSECs. **(E)** Flow cytometry analysis of CD31 and HbS in human primary lung endothelial cells. Representative IF images of Hb and CD31 localization in human primary lung endothelial cells (HMVECs-L). Scale bar 25 um. **(F)** Bar graph depicting the effect of Nystatin and latrunculin-A treatment in Hb uptake by LSECs. * denotes $p < 0.05$.

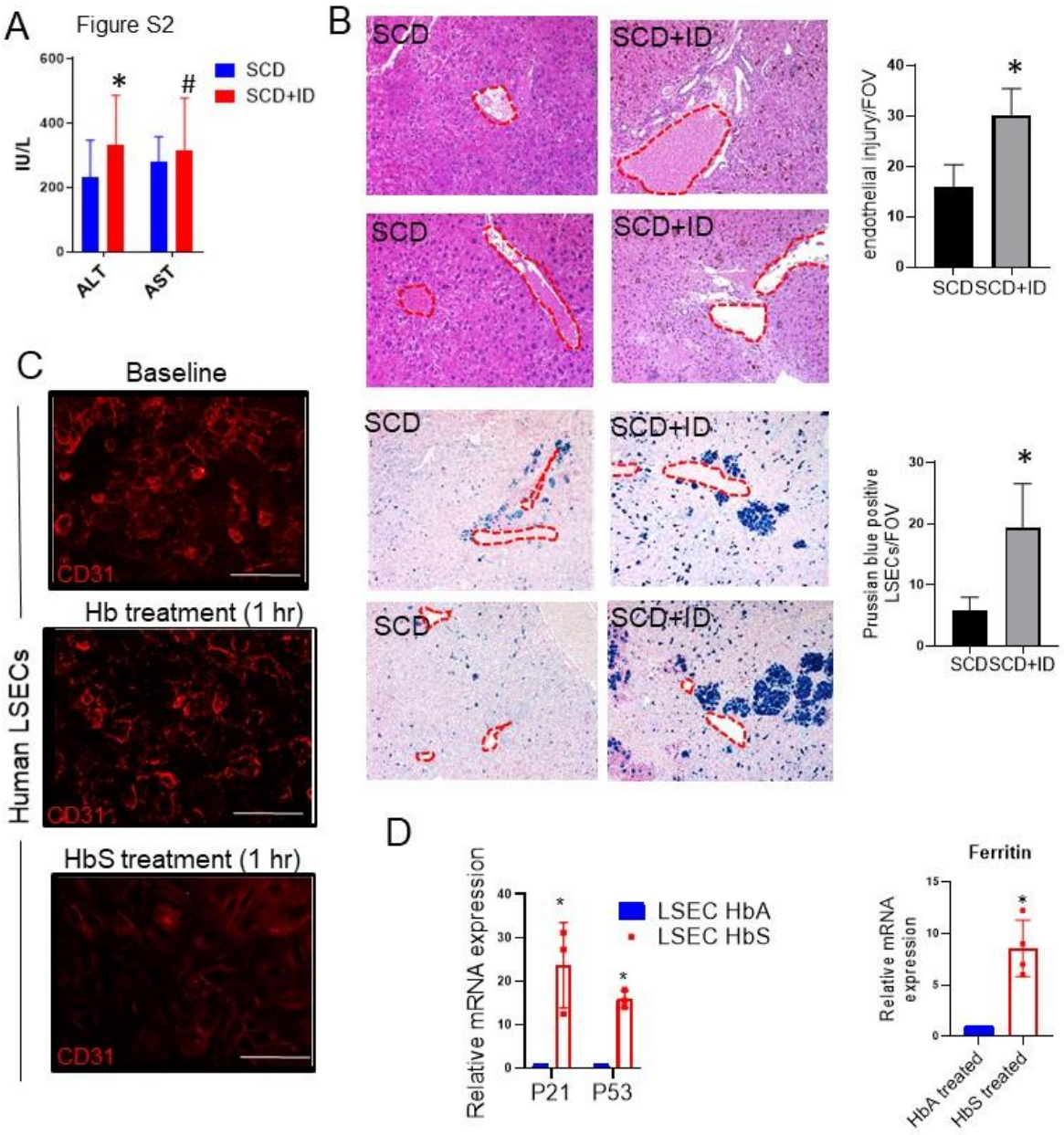
A
Figure S2
SCD
SCD+ID
IU/L
ALT
AST
B
SCD
SCD+ID
endothelial injury/FOV
Prussian blue positive LSECs/FOV
C
Baseline
Hb treatment (1 hr)
HbS treatment (1 hr)
Human LSECs
CD31
D
LSEC HbA
LSEC HbS
Relative mRNA expression
P21
P53
Ferritin
HbA treated
HbS treated
E
0 minute
15 minutes
30 minutes
1 hour
Hb-AF488
HbS-AF488

Figure S2: Accumulation of HbS and iron induces LSEC senescence. **(A)** Blood serum analysis shows significant increase in ALT and AST level post ID treatment in SCD mice compared to SCD mice at baseline. **(B)** Upper level: Representative H&E staining images showing exacerbated endothelial injury in iron dextran treated SCD mouse liver as compared to SCD mouse live at baseline. Endothelial cell and surrounding area is marked with dotted lines. Bar graph depicting the quantification of endothelial injury per field of view (FOV). Lower level: Representative Prussian blue staining images showing endothelial accumulation of iron in iron dextran treated SCD mouse liver as compared to SCD mouse live at baseline. Endothelial cell area is marked with dotted lines. Bar graph depicting the quantification of Prussian blue positive endothelial cells per field of view (FOV) * denotes $p < 0.05$. 100X zoomed in images are shown. **(C)** Representative IF images of CD31 positive human LSECs at baseline and post Hb and HbS treatment. Scale bar 25 um. **(D)** qRT-PCR analysis of senescence markers (P53 and P21) shows increased expression in HbS treated primary LSEC compared to Hb-A treated primary LSECs. qRT-PCR analysis of ferritin shows increased expression in HbS treated LSECs compared to Hb-A treated primary LSECs. **(E)** Representative IF images showing internalized Hb and HbS in human primary LSECs over time (0-1 hour). * denotes $p < 0.05$; ** denotes $p < 0.01$.

Figure S3

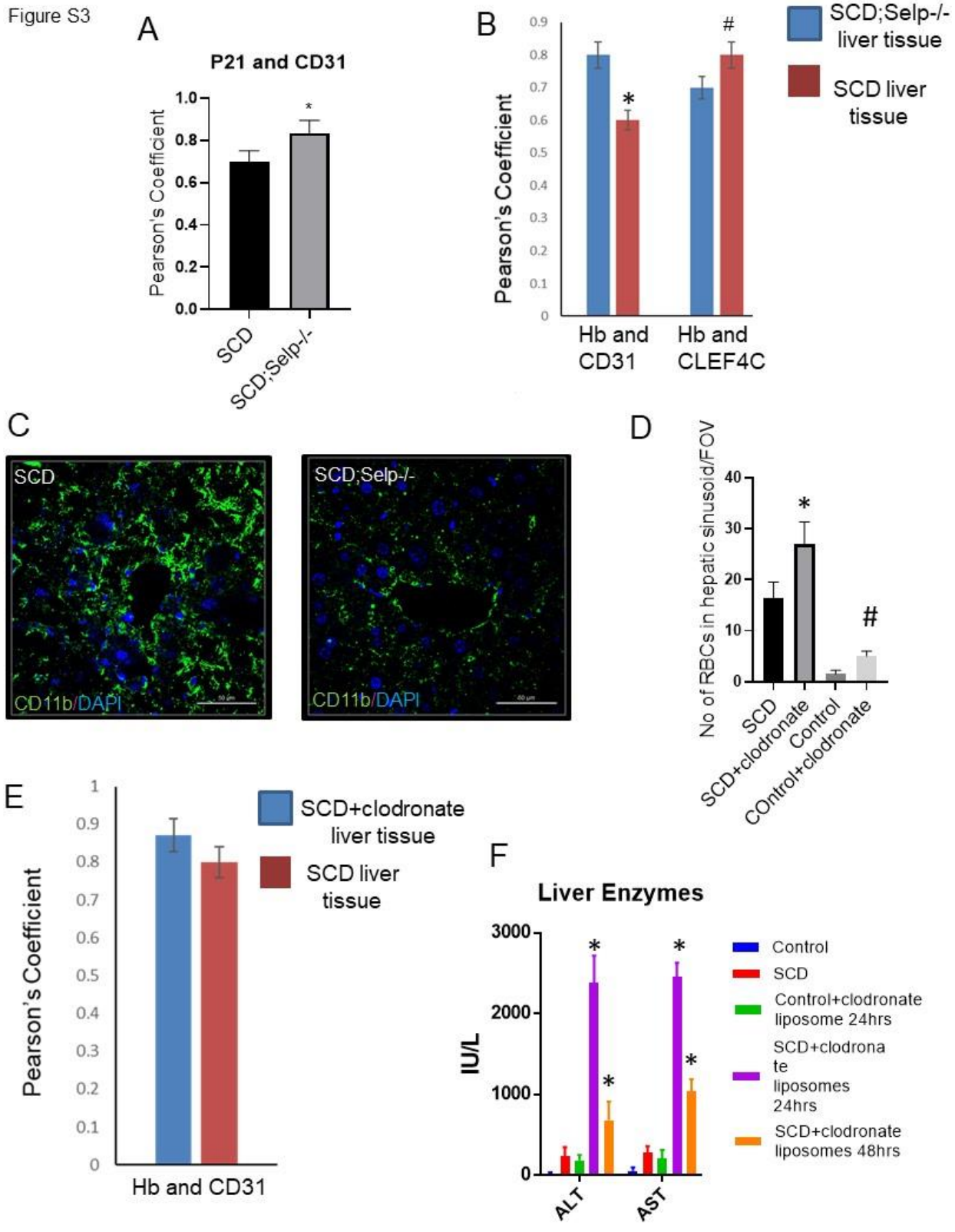

Figure S3: Loss of P-selectin and/ depletion of hepatic monocytes exacerbates LSEC senescence

and liver injury in SCD mice. Quantification of colocalization (by measuring Pearson's coefficient) observed in SCD and SCD;Selp-/- mouse liver tissue. **(A)** Bar graph shows the increased colocalization of P21 with LSEC marker CD31 and **(B)** hemoglobin with LSEC marker CD31 in SCD;Selp-/- mouse liver as compared to SCD mouse liver; * denotes $p < 0.05$. # denotes $p < 0.08$ **(C)** Representative IF images showing hepatic expression of monocyte marker CD11b in SCD and SCD;Selp-/- liver tissue. **(D)** Quantification of number of RBCs found in the hepatic sinusoids of SCD and control mice at baseline and after clodronate liposome treatment. * denotes $p < 0.05$. #<0.07. Scale bar 50 um. **(E)** Quantification of colocalization (by measuring Pearson's coefficient) observed in SCD mouse liver tissue at baseline and after clodronate liposome treatment. Bar graph shows the increased colocalization of hemoglobin with liver sinusoidal endothelial cell marker CD31 in clodronate-liposome treated SCD mouse liver as compared to SCD mice liver at baseline. p=0.074. **(F)** Blood serum analysis shows significant increase in ALT and AST level 24 and 48 hrs. post clodronate-liposome treatment in SCD liver. .* denotes $p < 0.05$. #<0.08. Scale bar 50 um.

Figure S4

A

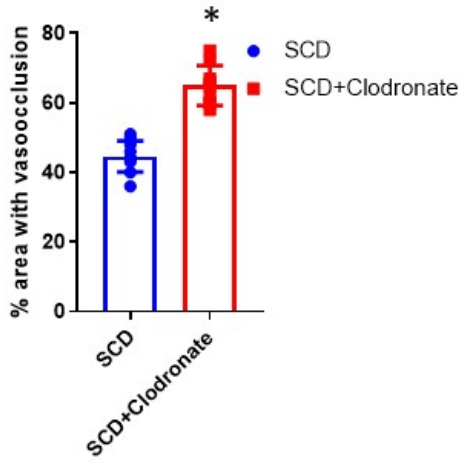

B

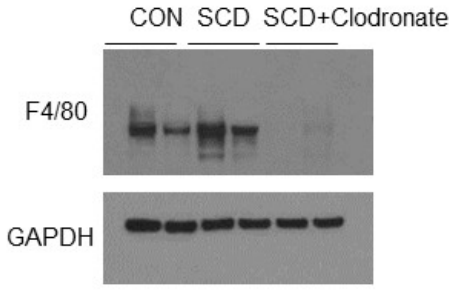

C

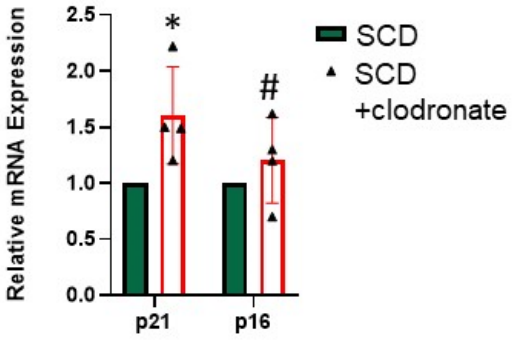

D

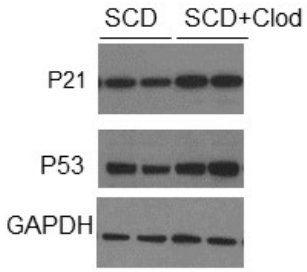

E

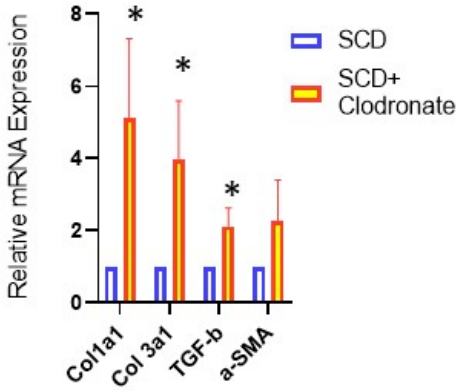

Figure S4: Depletion of hepatic Kupffer cells exacerbates LSEC senescence and liver injury in SCD mice. **(A)** Quantification of the area of vaso-occlusion in SCD mice at baseline and after clodronate treatment. The bar graph shows percentage of vaso-occlusion in each condition. (B)Western blot analysis of hepatic Kupffer cell marker F4/80 in SCD liver at baseline and post clodronate mediated macrophage depletion. **(C)** qRT-PCR analysis of senescence markers shows increased expression in SCD mice after clodronate mediated macrophage depletion compared to SCD mice at baseline. (D) Western blot analysis showing increased expression of senescence markers in SCD mice liver after clodronate mediated macrophage depletion. **(E)** qRT-PCR analysis shows increased transcriptional expression of liver injury markers in SCD mice liver after clodronate mediated macrophage depletion compared to SCD mice liver at baseline.

Supplemental Video Legends:

Movie S1-2. Visualization of blood flow in a wildtype mouse after administration of TXR-dextran and P21 prior to imaging. The sinusoids in WT young (3 months old) liver visualized by carotid artery injection of TXR-dextran (red) and P21 (green; as a marker for senescent cells). Original acquisition rate. Scale bar 20 uM.

Movie S3-4. Visualization of blood flow in a SCD mouse after administration of TXR- dextran and P21 prior to imaging. The sinusoids in WT young (3 months old) liver visualized by carotid artery injection of TXR-dextran (red) and P21 (green; as a marker for senescent cells). P21staining is enriched in liver sinusoidal endothelial cell like structure. Original acquisition rate. Scale bar 20 uM.

Movie 5-6 Visualization of blood flow in a SCD; SelP-/- mouse after administration of TXR-dextran and P21 prior to imaging. The sinusoids in WT young (3 months old) liver visualized by carotid artery injection of TXR-dextran (red) and P21 (green; as a marker for senescent cells). P21staining is enriched in liver sinusoidal endothelial cell like structure. Original acquisition rate. Scale bar 20 uM.

Movie S7-8: Visualization of blood flow in a clodronate liposome treated SCD mouse after administration of TXR- dextran prior to imaging. The sinusoids in SCD mouse liver visualized by carotid artery injection of TXR-dextran (red) after clodronate liposome treatment . Sinusoidal vaso-occlusion was seen as dark regions without any flow of blood. Original acquisition rate. Scale bar 20 uM.